cells

MDPI

Supplementary Materials:

Functional Characterization of Clinically-Relevant Rare Variants in *ABCG2* Identified in a Gout and Hyperuricemia Cohort

Yu Toyoda [1], Andrea Mančíková [2], Vladimír Krylov [2], Keito Morimoto [1], Kateřina Pavelcová [3], Jana Bohatá [3], Karel Pavelka [3], Markéta Pavlíková [5], Hiroshi Suzuki [1], Hirotaka Matsuo [4], Tappei Takada [1] and Blanka Stiburkova [3,6,*]

[1] Department of Pharmacy, The University of Tokyo Hospital, Tokyo 113-8655, Japan; ytoyoda-tky@umin.ac.jp (Y.T.), kmorimoto-tky@umin.ac.jp (K.M.), suzukihi-tky@umin.ac.jp (H.S.), tappei-tky@umin.ac.jp (T.T.)
[2] Department of Cell Biology, Faculty of Science, Charles University, 128 00 Prague 2, Czech Republic; andrea.mancikova@email.cz (A.M.), vladimir.krylov@natur.cuni.cz (V.K.)
[3] Institute of Rheumatology, 128 50 Prague 2, Czech Republic; pavelcova@revma.cz (Kat.P.), bohata@revma.cz (J.B.), pavelka@revma.cz (Kar.P.), stiburkova@revma.cz (B.S.)
[4] Department of Integrative Physiology and Bio-Nano Medicine, National Defense Medical College, Saitama 359-8513, Japan; hmatsuo@ndmc.ac.jp (H.M.)
[5] Department of Probability and Mathematical Statistics, Faculty of Mathematics and Physics, Charles University, 121 16 Prague 2, Czech Republic; pavlikova@karlin.mff.cuni.cz (M.P.)
[6] Department of Pediatrics and Adolescent Medicine, First Faculty of Medicine, Charles University and General University Hospital, 121 08 Prague 2, Czech Republic
* Correspondence: stiburkova@revma.cz; Tel.: +420-234-075- 319 (B.S.)

Received: 20 March 2019; Accepted: 15 April 2019; Published: date

1. Supplemental Methods

1.1. Sub-cloning and in vitro Transcription

Using the GeneArt™ Site-Directed Mutagenesis System and AccuPrime™ Pfx DNA Polymerase (Invitrogen, Carlsbad, CA, USA), vectors for *in vitro* transcription of different ABCG2 variants were generated from the full-length ABCG2 wild-type (WT) open reading frame (ORF) inserted in the pCMV6-AC vector (ORIGENE, Rockville, MD, USA). Appropriate cRNAs were prepared using an Invitrogen™ Ambion™ mMESSAGE mMACHINE™ T7 Transcription Kit (Invitrogen) and stored at −80 °C until used. In a similar manner, the cRNA of URAT1 (NM_144585.3) was obtained from the full-length URAT1 WT ORF inserted in the pcDNA 3 vector (Thermo Fisher, Vilnius, Lithuana). Before *in vitro* transcription, template plasmids were linearized using *Not* I.

1.2. Preparation of URAT1 and ABCG2 Expressing Oocytes

Female *Xenopus laevis* was anesthetized in a 0.1% ethyl 3-aminobenzoate methanesulfonate solution (Sigma-Aldrich, Steinheim, Germany) and then transferred on ice. After surgical incision, part of the ovary was cut from the abdominal cavity. To obtain defolliculated oocytes, extracted oocytes were treated with 2 mg/mL Collagenase A (Sigma-Aldrich) in a Ca^{2+}-free OR2 solution (82.5 mM, 2.5 mM KCl, 2.5 mM $CaCl_2$, 1 mM $MgCl_2$, 5 mM HEPES, and pH 7.4) for 90 min at 18 °C with gentle shaking, and then washed in fresh OR2 solution. Under stereomicroscpic observation, only oocytes with a diameter > 1 mm (at stages V–VI) were transferred to ND-96 solution (96 mM NaCl, 2mM KCl, 1.8 mM $CaCl_2$, 1 mM $MgCl_2$, 5 mM HEPES, and pH 7.5) for subsequent microinjection. Using a pneumatic microinjector (Narishige, Tokyo, Japan), 50 ng of cRNA was injected into each oocyte and the oocytes were subjected to further incubation at 18 °C.

1.3. Urate Transport Assay in Xenopus Oocytes

Urate transport assay in *Xenopus leavis* oocytes was carried out according to the methods describe in a previous study [S1]. In brief, two days after cRNA injection, intact oocytes were transferred into an ND-96 solution (a standard incubation buffer for oocyte uptake assay) containing 600 μM radiolabeled uric acid ([8-^{14}C]-uric acid; American Radiolabeled Chemicals, St. Louis, MO, USA). After incubation for 30 min at 18 °C, oocytes were washed in cold ND-96 solution three times, and then lysed using 1N NaOH and neutralized using 2N HCl in scintillation tubes. In an Ultima Gold™ scintillation cocktail (SigmaAldrich), radioactivities of oocytes that had incorporated radiorabeled urate were measured using a Hewlett Packard Liquid Scintillator (TRI-CARB 2900TR, PerkinElmer, Downers Grove, IL, USA). Uptake of uric acid was analyzed for 30 oocytes in total for each allelic variant.

1.4. Statistical Analysis

Data from the oocyte uptake assay were analyzed by one-way analysis of variance (ANOVA) and differences between groups (ABCG2 WT *vs* each allelic variant) were examined through a two-sample *t*-test. Statistical significance was defined in terms of *P* values less than 0.05 or 0.01.

2. Supplemental Results

2.1. Urate Uptake in Xenopus Oocytes Expressing URAT1 and ABCG2

In this assay, each ABCG2 variant was co-expressed with URAT1 WT that was used for the enhancement of urate uptake into oocytes. To estimate the urate efflux ability of each ABCG2 variant, the net accumulation of radiolabeled urate into the URAT1 WT/ABCG2 double-expressing oocytes was examined for 30 min in ND-96 solotion. As expected, among the tested groups, only URAT1 WT-expressing oocytes had the maximum capacity for urate accumulation and URAT1 WT/ABCG2 WT-expressing oocytes showed the lowest capacity for urate accumulation (**Supplemental Figure S1**). The results suggest that oocytes expressing seven ABCG2 variants (T434M, S474P, T153M, F373C, Q141K, R147W, and S572R) could have lower capacity for urate efflux compared with oocytes expressing ABCG2 WT.

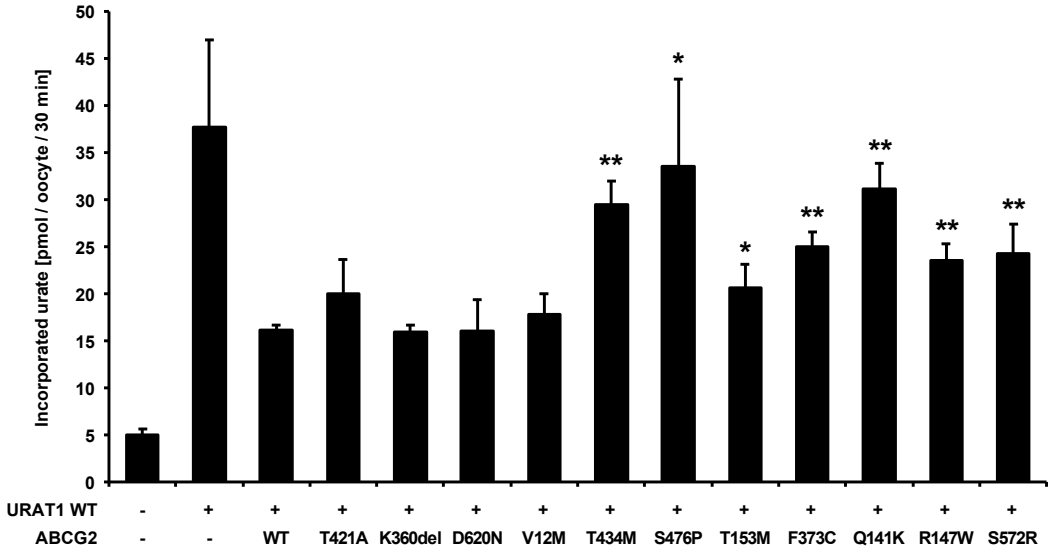

Supplemental Figure S1. Urate accumulation in *Xenopus oocytes* expressing URAT1 WT and ABCG2 variants after a 30 min incubation in ND-96 solution containing 600 μM radiolabeled uric acid. In the oocytes expressing seven variants, higher urate accumulation was detected compared with ABCG2 WT. *, $P < 0.05$; **, $P < 0.01$.

Supplemental Table S1

Supplemental Table S1. Medication and number of allelic variants in the gout and hyperuricemia cohorts.

Characteristic	All patients (*N* = 250)		Gout (*N* = 182)		Hyperuricemia (*N* = 68)		*P*-value[#]
	N	%	*N*	%	*N*	%	
Medication							
Nothing	58	23.2	28	15.4	30	44.1	0.0000
Allopurinol	175	70.0	137	75.3	38	55.9	
Febuxostat	17	6.8	17	9.3	0	0.0	
Number of Q141K							
0	147	58.8	103	56.6	44	64.7	0.3682
1	87	34.8	68	37.4	19	27.9	
2	16	6.4	11	6.0	5	7.4	
Number of V12M							
0	241	96.4	174	95.6	67	98.5	0.4511
1	9	3.6	8	4.4	1	1.5	
At least one variant							
0	135	54.0	92	50.5	43	63.2	0.0873
1 or 2	115	46.0	90	49.5	25	36.8	
Number of variants							
0	135	54.0	92	50.5	43	63.2	0.1121
1	92	36.8	74	40.7	18	26.5	
2	23	9.2	16	8.8	7	10.3	

[#] Fisher's exact test was used to compare the gout cohort with the hyperuricemic cohort in terms of the use of medication, Q141K and V12M genotype distribution, and the number/presence of 11 studied allelic variants. There was no patient with three or more non-synonymous variants in *ABCG2*.

Supplemental Figure S2

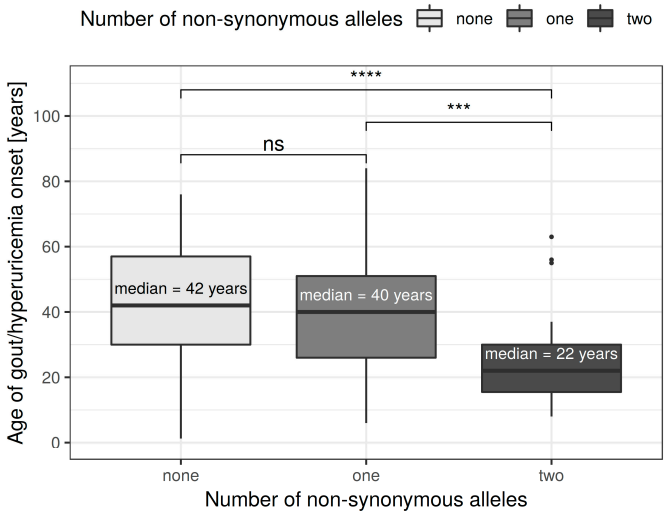

Supplemental Figure S2. Onset of gout/ age of ascertainment of hyperuricemia and the numbers of allelic variants in *ABCG2*. According to the number of the 11 non-synonymous alleles identified in *ABCG2*, information on onset age was summarized as a box-and-whiskers plot. Based on the Kruskal-Wallis test, there were significant differences among groups ($P < 0.0002$); post-hoc comparisons (pairwise Wilcoxon tests with Bonferroni correction) showed significant differences between the two-allele group and both none- and one-allele groups. ***, $P < 0.001$; ****, $P < 0.0001$; ns, not significantly different between groups.

Supplemental Figure S3

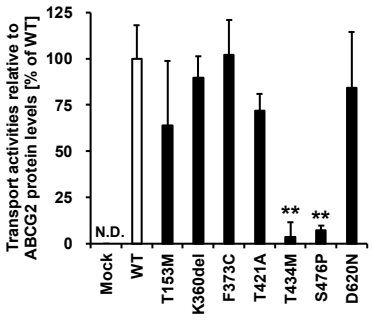

Supplemental Figure S3. Urate transport activities relative to ABCG2 protein levels. ABCG2 protein levels were determined semi-quantitatively by immunoblotting. For this purpose, the signal intensity ratio (ABCG2/ Na^+/K^+ ATPase) of the immunoreactive bands shown in Figure 5A was determined and normalized to that in ABCG2 WT-expressing cells. The data are shown as % of WT; data are expressed as the mean ± SD. $n = 3$. Statistical analyses for significant differences were performed using Bartlett's test, followed by a Dunnett's test (*, $P < 0.05$; **, $P < 0.01$ *vs* WT). N.D., not determined.

Supplemental Figure S4

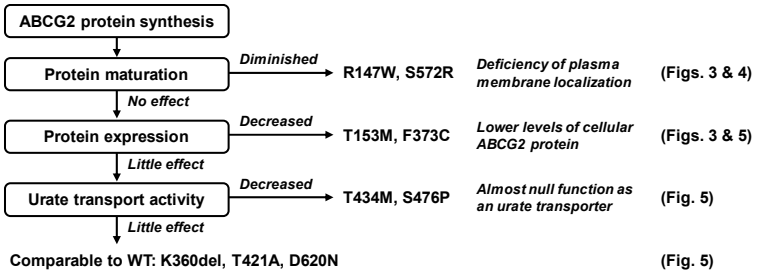

Supplemental Figure S4. Schematic illustration of the effects of each rare mutation we studied on the intracellular processing and function of ABCG2 protein.